A STREAMLINE DIFFUSION METHOD FOR A NONLINEAR EQUATION GOVERNING THE SPREADING OF OIL SPILLS

Márcio Rodolfo Fernandes
fernands@mtm.ufsc.br
Universidade Federal de Santa Catarina, Departamento de Matemática - CFM
CEP 88040-900 - Florianópolis, SC, Brazil
Petronio Pulino
pulino@ime.unicamp.br
José Luiz Boldrini
boldrini@ime.unicamp.br
Universidade Estadual de Campinas, IMECC
C.P. 6065 - 13083-970 - Campinas, SP, Brazil

Abstract

The paper describes a finite element method that uses a version of the space-time streamline diffusion technique and includes the control of total mass applied to a nonlinear convection–diffusion equation that governs the spreading of oil spills on moving water surfaces. The use of such equation for numerical predictions of the evolution of such spills, although highly desirable to help to lessen their consequences, brings several difficulties. In fact, from the theoretical point of view, the equation presents either parabolic or hyperbolic (in the sense of transport equations) character depending on the solution itself. This is due to the nonlinearity of the diffusion term that can pass from strictly positive to zero and vice-versa depending on the value of the

solution. In such *a priori* unknown regions, fast transitions may occur, bringing spurious oscillations that may deteriorate the numerical solutions obtained with ordinary algorithms. The performance of the proposed method is compared in controled situations with the corresponding performances of more traditional methods. The results shows clear advantages in its use.

Keywords: Oil spills, Finite elements, Streamline diffusion, Mass control.

1 INTRODUCTION

In this work we are interested in describing a numerical method that combines streamline diffusion and discontinuous Galerkin techniques, and it will be applied to an equation governing the spreading of oil spills on moving water surfaces (see Benqué, Hauguel & Viollet [1]):

$$\frac{\partial u(x,t)}{\partial t} - c\Delta(u^3(x,t)) + \vec{\beta}(x,t)\cdot\nabla u(x,t) = f(x) \ \ , \ \ \Omega \times I \tag{1}$$

$$u(x,t) = g(x,t) \ , \ x \in \ \partial\Omega_- \ , \ \ t \in I \tag{2}$$

$$\frac{\partial u(x,t)}{\partial \vec{\eta}} = 0 \ , \ \ x \in \ \partial\Omega_+ \ , \ \ t \in I \tag{3}$$

$$u(x,0) = u_0(x) \ , \ x \in \Omega. \tag{4}$$

Here, Ω denotes the region of interest, which is assumed to be a bounded domain in $I\!R^2$ with Lipschtz boundary denoted by $\partial\Omega$; the unitary external normal at $x \in \partial\Omega$ is denoted $\vec{\eta}(x)$; $I = (0,T] \subset I\!R$, with $T > 0$ being the final time of interest; u denotes the (normalized) height of the spill measured from the water surface; $\vec{\beta}$ is the driving velocity field, which according to [1] is a combination of the water and wind velocities, and for simplicity we assume to be *a priori* known divergence free field (in realistic situations, this field should be previously computed using another numerical scheme for Navier-Stokes equations, for instance); $c > 0$ is a positive coefficient associated to the nonlinear diffusion and depending on the physical properties involved; f denotes the aggregated effects of several other factors like possible external sources/sinks of oil; $u_0(\cdot)$ denotes the initial distribution of the spill.

The boundary $\partial\Omega$ will be considered to be composed of tree disjoint parts: the physical walls, denoted by $\partial\Omega_0$, where the velocity field $\vec{\beta}$ is usually null,

and the outlet and inlet parts, given respectively by

$$\partial\Omega_+(t) = \{\ x \in \partial\Omega - \partial\Omega_0\ :\ \vec{\eta}(x)\cdot\vec{\beta}(x,t) \geq 0\ \},$$

$$\partial\Omega_-(t) = \{\ x \in \partial\Omega - \partial\Omega_0\ :\ \vec{\eta}(x)\cdot\vec{\beta}(x,t) < 0\ \}.$$

Here, "$\cdot$" is the usual inner product in $\mathbb{R}^2$. $g(\cdot,\cdot)$ is the possible flux of oil coming from $\partial\Omega_-$.

Mathematical properties of the previous equation, like the conservation of compact support of solutions, can be found for instance in Bertsch [2].

We should stress that, since oil spills are nowadays important environmental hazards, accurate and reliable predictions about their behavior are in much need, bringing the necessity of using improved mathematical models for their spreading. The previous nonlinear equation models the important physical mechanisms involved in the spreading of such spills in a much better way than the usual linear models, and therefore results derived from it should be useful.

However, the use of (1) for numerical predictions, although highly desirable, brings new difficulties. In fact, from the theoretical point of view, equation (1) has characteristics that may be either parabolic or hyperbolic (in the sense of transport equations), and which is not *a priori* known. In fact, due to the nonlinear character of the diffusion term, it depends on the solution itself, passing from strictly positive to zero depending on the value of u. Fast transitions can occur in u, bringing spurious oscillations that may deteriorate the numerical solutions obtained by usual technique. This brings the necessity of using numerical methods with increased stability.

Another important aspect to consider is that usually oil spills occur in regions with irregular boundaries (like most coastal lines). Such geometrical difficulties make harder to use finite differences schemes to numerically solve the problem. For this reason, in this paper we consider numerical methods based on a finite elements, which are naturally adapted to such varied geometries.

The last two remarks suggest the use of finite elements methods with increased stability. However, it will be necessary that not to much artificial dissipation be introduced as an exchange for stability. There are several reasonable ways to try to obtain that. For instance, one could discretize the time variable using a backward Euler scheme, and then use finite elements to discretize the spatial variables, with the help of the streamline diffusion technique or the use of bubble functions to stabilize the resulting scheme

(see Section 2 for details). As we will show later on, these procedures can reduce the numerical difficulties associated to spurious oscillations, although not yet in a totally satisfactory way. We will see that a better way is to use streamline diffusion in space and time, working with two levels of time at each step. However, these three methods do not behave well with respect to the important property of balance (conservation) of total mass that equation (1) has to satisfy. Therefore, in this paper we propose a version of the last method including a method to control of total mass.

We should stress that the purpose of this paper is not to show realistic and complex simulations of oil spills; this will be the subject of future work. Our objetive here is to introduce the method and compare it with more standard ones. For this, it is necessary to experiment in rather simple and controled situations, where objective comparations criteria can be used. This is done in Section 4, where three numerical experiments are described (one of them is a situation having an exact solution.) The results show that the proposed method is rather satisfactory as compared to the usual ones.

2 FINITE ELEMENT METHODS WITH INCREASED STABILITY

There are several possible combinations between linearization procedures and discretization applied to Problem (1)–(4). Here, we briefly describe some simple, frequently used possibilities.

We start by discretizing the time variable using finite differences (backward Euler) and the spatial variable using usual finite elements. The linearization can then be done simply by taking profit of the discretization of the time variable by suitable delaying of the coefficients. In some details, let $\Pi: \quad 0 = t_0 < t_1 < \cdots < t_N = T$ be a fixed partition of $I = [0, T]$; denote $I_n = (t_{n-1}, t_n)$ and the local time step by $k_n = t_n - t_{n-1}$. The nonlinear term $\Delta(u^3(x,t))$ can be rewritten as

$$\Delta(u^3(x,t)) = \text{ div } (\nabla u^3(x,t)) = \text{ div } (3u^2(x,t)\nabla u(x,t)). \tag{5}$$

Now, being $u^n(x)$ an approximation of $u(x, t_n)$, $n = 1, 2, \cdots, N$, at each time t_n we can approximate (5) by computing $u^2(x,t)$ at the previous time step. Thus, we have to solve a linear problem at each time step: we have to

find $u^n(x)$, $n = 1, 2, \cdots, N$, $x \in \Omega$ satisfying

$$\frac{u^n - u^{n-1}}{k_n} - \text{ div } (3c(u^{n-1})^2 \nabla u^n) + \vec{\beta}(x,t) \cdot \nabla u^n = f(x), \tag{6}$$

$$u^0(x) = u_0(x). \tag{7}$$

The corresponding variational formulation of problem (6), (7) with boundary condition (2), (3) can be obtained as follows. Define, respectively, the functional space of the test-functions and the functional space of approximations, that is the space where the solution must be located:

$$H_0^1 = \{v \in \mathcal{H}^1(\Omega) \ / \ v \mid_{\partial\Omega_-} = 0\};$$

$$H_g^1 = \{ \ v \in \mathcal{H}^1(\Omega) \ / \ v \mid_{\partial\Omega_-} = g \ \};$$

then multiply (6) by $v \in H_0^1$ and integrate the result on Ω; use Green's theorem to get the following variational problem

$(\mathcal{V}_g)$ find $u^n \in H_g^1$, $n = 1, 2, \cdots, N$, such that

$$\langle u^n, v \rangle + k_n a(u^n, v) = b(v), \forall \ v \in H_0^1, \tag{8}$$

$$u^0(x) = u_0(x), \tag{9}$$

where

$$a(u^n, v) = \int_\Omega 3c(u^{n-1}(x))^2 \nabla u^n(x) \cdot \nabla v(x) dx + \int_\Omega \vec{\beta}(x,t) \cdot \nabla u^n(x) v(x) dx,$$

$$b(v) = \langle k_n f + u^{n-1}, v \rangle = \int_\Omega k_n f(x) v(x) dx + \int_\Omega u^{n-1}(x) v(x) dx,$$

$$\langle u^n, v \rangle = \int_\Omega u^n(x) v(x) dx.$$

The traditional finite elements formulation is derived from the above by considering a small parameter $h > 0$ associated to the size of used mesh, and a suitable poligonal domain Ω_h approximating Ω. Then, one considers, for instance, the finite dimensional functional space $V_h \subset H_0^1$ given by

$$V_h = \{ \ v \in H_0^1 \ / \ v \mid_K \in \mathcal{P}_r(K), \forall \ K \in T_h \ \},$$

and $V_h^g \subset H_g^1$ defined by

$$V_h^g = \{ \ v \in H_g^1 \ / \ v \mid_K \in \mathcal{P}_r(K), \forall \ K \in T_h \ \},$$

where $T_h = \{K\}$ is a triangularization of Ω_h, with triangles of size of order h, and $\mathcal{P}_r(K)$ is the space of polynomials of degree less than or equal to $r \in N$, defined on K.

The finite elements formulation of the above problem then becomes

$(\mathcal{V}_h)$ Find $u_h^n \in V_h^g,\ n = 1, 2, \cdots N$, such that

$$\langle u_h^n, v\rangle + k_n a(u_h^n, v) = b(v), \quad \forall\ v \in V_h, \tag{10}$$

$$\langle u_h^0, v\rangle = \langle u_0, v\rangle, \ \ \forall\ v \in V_h. \tag{11}$$

Being $\{\Psi_1, \Psi_2, \cdots, \Psi_M\}$ a basis for V_h, for each n we can write $u_h^n(x) = \sum_{j=1}^M c_j^n \Psi_j(x)$, and thus the last problem is equivalent to the following linear system of M equations and M variables $c_1^n, c_2^n, \cdots, c_M^n$

$$\mathbf{A(c^{n-1})c^n} = \mathbf{Bc^{n-1}} + \mathbf{d^{n-1}}. \tag{12}$$

We remark that at each step of time, the matrix depends on the solution computed at the previous time, as it is shown above by the indication of its dependence on the coefficients $\mathbf{c^{n-1}}$.

One usually expects to obtain control of the L^2-norms of the approximate solution and of its first derivatives. In the above problem, however, when the diffusion term $3c(u^{n-1})^2$ becomes small, the control over L_2-norm of ∇u_h^n is lost. This happens in particular when u_h^n has compact support, and there are regions where the diffusion coefficient decreases to zero. In such regions the problem becomes purely hyperbolic and the above tradicional formulation does not work due to the appearance of oscilations in the approximate solution. In the following, we describe two ways to reduce these difficulties.

One way to do this is to change the functional space of test-functions (such techniques receive the general name of Petrov-Galerkin methods.) The streamline diffusion method is one of them and is based in taking test-functions of form $v + \delta\vec{\beta}\cdot\nabla v\ ,\ \ v \in V_h$ in place of just v in (10), (11). In an extended form this furnishes the following procedure, which we call **Euler-Streamline Diffusion Method**, or **E-SD** for short:

$$\begin{aligned}
&\langle \frac{u_h^n - u_h^{n-1}}{k_n}, v + \delta\vec{\beta}\cdot\nabla v\rangle + \langle 3c(u^{n-1})^2\nabla u_h^n, \nabla v\rangle \\
&- \langle\ \mathrm{div}\ (3c(u^{n-1})^2\nabla u_h^n), \delta\vec{\beta}\cdot\nabla v\rangle + \ \langle\vec{\beta}\cdot\nabla u_h^n, v + \delta\vec{\beta}\cdot\nabla v\rangle \\
&= \ \langle f, v + \delta\vec{\beta}\cdot\nabla v\rangle, \quad \forall\ v \in V_h, \ \ n = 1, 2, \cdots, N. \\
&\langle u_h^0, v + \delta\vec{\beta}\cdot\nabla v\rangle = \langle u_0, v + \delta\vec{\beta}\cdot\nabla v\rangle,\ \forall\ v \in V_h.
\end{aligned} \tag{13}$$

Here, $\delta = \overline{c}h$, with $\overline{c} > 0$ sufficiently small, when $3c(u^{n-1})^2 < h$; $\delta = 0$ when $3c(u^{n-1})^2 \geq h$.

We observe that the term $\delta\langle\vec{\beta}\cdot\nabla u_h^n, \vec{\beta}\cdot\nabla v\rangle$ may be interpreted as a diffusive transport in the direction of the flow $\vec{\beta}$; it works as a stabilization factor for the numerical scheme because increases the amount of diffusivity in the flow direction without violating consistency.

Further details concerning this method can be found for instance in Johnson citeJohnson1987.

A second idea to improve stabilization is to work with a larger approximation space V_h by the inclusion of the so called bubble functions, which are basically functions with support in each element; see for instance Franca & Farhat [4]. As an example of such larger approximation space, we could take it consisting the space generated by the linear combinations of polynomial by parts functions (degree 1, for instance) and cubic bubbles:

$$V_h^b = \{\ v \in H_0^1\ /\ v\mid_K \in \mathcal{P}_r(K) \oplus \mathcal{B}(K),\ \forall K \in T_h\ \},$$

where $\mathcal{B}(K)$ is the space of bubble functions defined on each element $K \in T_h$.

Proceeding as before, we arrive at the following procedure, which we call **Euler-Galerkin with Bubble Functions**, or **E-GBF** for short: we have to find $u_h \in V_h^b$ such that for all $v \in V_h^b$

$$\begin{aligned} &\langle\frac{u_h^n - u_h^{n-1}}{k_n}, v\rangle + \langle 3c(u^{n-1})^2\nabla u_h^n, \nabla v\rangle + \langle\vec{\beta}\cdot\nabla u_h^n, v\rangle = \langle f, v\rangle, \\ &\langle u_h^0, v\rangle = \langle u_0, v\rangle. \end{aligned} \tag{14}$$

As we show later on, the last two methods are have enough stability to control the wild oscillations presented by the standard method. However, they still present too much artificial diffusivity for the problem at hand, and lead to excessive spreading and decaying of solution.

3 SPACE-TIME STREAMLINE DIFFUSION METHOD AND CONTROL OF MASS

A different form of discretizing (1)–(4) is the following. We still use the same sort of linearization procedure, but, instead of using finite differences in the time variable and then some sort of Galekin procedure for the spatial variables, we will use the Galekin procedure simultaneously in space and

time. That is, we use finite elements and interpolation functions depending on time and space. Space-time streamline-diffusion can be used to improve stabilization; however, used without care, this would lead to a very large linear system to be solved. The reason for this is that in this technique the use of continuous (in time) test-functions couple all levels of time. One way to avoid this difficulty, and decrease the size of the corresponding linear system, is to work in strips of space-time, with the help of interpolation functions that will be continuous in the spatial variables, but will be descontinuous in the time variables at the common frontier of every two strips. In the following, we give some details.

Adapting ideas of Johnson [5] to our nonlinear problem, we take as before a partition $\Pi : \quad 0 = t_0 < t_1 < \cdots < t_N = T$ of $I = [0, T]$, and for each $n = 1, 2, \cdots, N$ we will work in strips of space-time S_n given by

$$S_n = \{(x, t) \ : \ x \in \Omega, \ t_{n-1} < t < t_n\}.$$

Let V_h^n be a fixed finite element subspace in $\mathcal{H}^1(S_n)$, where h is a parameter as before, and let

$$V_h^{0n} = \{v \in V_h^n \ / \ v(x, t) = 0, x \in \partial\Omega_-\}.$$

In this version of streamline diffusion, we work in space-time, using test-functions of form

$$v + \delta(\frac{\partial v}{\partial t} + \vec{\beta} \cdot \nabla v), \tag{15}$$

where

$$\delta = \overline{c}h, \tag{16}$$

and $\overline{c} > 0$ is a positive constante.

Multiplying the equation by the above test-function and integranting successively on each strip S_n, with the help of integration by parts, and weakly imposing as initial condition for $t = t_{n-1}$ the value of u^{n-1} computed at the previous strip and strongly imposing the boundary conditions, we obtain a procedure that we call **Space-Time Streamline Diffusion**, or **S-T-SD** for short:

$(\mathcal{V}_h)$ Find $u_h^n \in V_h^{0n}, \ n = 1, 2, \cdots N$, such that for all V_h^{0n} there holds

$$\begin{aligned} &\langle \frac{\partial u_h^n}{\partial t} + \vec{\beta} \cdot \nabla u_h^n, v + \delta(\frac{\partial v}{\partial t} + \vec{\beta} \cdot \nabla v)\rangle^n + \langle 3c(u_-^{n-1})^2 \nabla u_h^n, \nabla v\rangle^n \\ &- \langle \text{ div } (3c(u_-^{n-1})^2 \nabla u_h^n), \delta(\frac{\partial v}{\partial t} + \vec{\beta} \cdot \nabla v)\rangle^n + \langle\langle u_{h+}^n, v_+\rangle\rangle^{n-1} \\ &= \ \langle f, v + \delta(\frac{\partial v}{\partial t} + \vec{\beta} \cdot \nabla v)\rangle^n + \langle\langle u_{h-}^{n-1}, v_+\rangle\rangle^{n-1}. \end{aligned} \tag{17}$$

Here, for simplicity of exposition, we took $g \equiv 0$ in (2); as before, $\delta = \overline{c}h$ when $3c(u_-^{n-1})^2 < h$, where $\overline{c} > 0$ sufficiently small; $\delta = 0$ when $3c(u_-^{n-1})^2 \geq h$. Moreover, we take $u_-^0 = u_0$ and use the following notations

$$\langle w, v \rangle^n = \int_{S_n} w(x,t)v(x,t)dxdt,$$

$$\langle\langle w, v \rangle\rangle^n = \int_{\Omega} w(x,t_n)v(x,t_n)dxdt,$$

$$v_+(x,t) = \lim_{s \to 0^+} v(x,t+s),$$

$$v_-(x,t) = \lim_{s \to 0^-} v(x,t+s).$$

To describe the space-time basis of finite elements that will be considered, let $\{\Psi_1, \Psi_2, \cdots, \Psi_M\}$ be the following basis for V_h:

$$V_h = \{\ v \in H_0^1 \ / \ v\ |_K \in \mathcal{P}_r(K), \forall\ K \in T_h\ \}.$$

Take $\{\lambda_1, \lambda_2\}$ as the basis for the space of polynomial functions of degree at most one and defined on the interval (t_{n-1}, t_n):

$$\lambda_1(t) = \frac{t_n - t}{t_n - t_{n-1}}, \quad \lambda_2(t) = \frac{t - t_{n-1}}{t_n - t_{n-1}}.$$

We can construct $\{\Phi_1, \Phi_2, \cdots, \Phi_{2M}\}$ para V_h^{0n} as:

$$\Phi_1(x,t) = \lambda_1(t)\Psi_1(x),\ \Phi_2(x,t) = \lambda_1(t)\Psi_2(x),\ \cdots, \Phi_M(x,t) = \lambda_1(t)\Psi_M(x),$$

$$\Phi_{M+1}(x,t) = \lambda_2(t)\Psi_1(x),\ \Phi_{M+2}(x,t) = \lambda_2(t)\Psi_2(x),\ \cdots, \Phi_{2M}(x,t) = \lambda_2(t)\Psi_M(x).$$

Therefore, being the approximate solution on S_n given by $u_h^n(x,t) = \sum_{j=1}^{2M} c_j^n \Phi_j(x,t)$, (17) is equivalent to the following system of order $2M$ for the coefficients c_j^n:

$$\sum_{j=1}^{2M} c_j^n \left[\langle \frac{\partial \Phi_j}{\partial t} + \vec{\beta} \cdot \nabla \Phi_j, \Phi_i + \delta(\frac{\partial \Phi_i}{\partial t} + \vec{\beta} \cdot \nabla \Phi_i) \rangle^n + \langle 3c(\sum_l c_l^{n-1}\Phi_l)^2 \nabla \Phi_j, \nabla \Phi_i \rangle^n \right]$$
$$+ \sum_{j=1}^{2M} c_j^n \left[- \langle\ \text{div}\ (3c(\sum_l c_l^{n-1}\Phi_l)^2 \nabla \Phi_j), \delta(\frac{\partial \Phi_i}{\partial t} + \vec{\beta} \cdot \nabla \Phi_i) \rangle^n + \langle\langle \Phi_{j+}, \Phi_{i+} \rangle\rangle^{n-1} \right]$$
$$= \sum_{j=1}^{2M} c_j^{n-1} \left[\langle\langle \Phi_{j-}, \Phi_{i+} \rangle\rangle^{n-1} \right] + \langle f, \Phi_i + \delta(\frac{\partial \Phi_i}{\partial t} + \vec{\beta} \cdot \nabla \Phi_i) \rangle^n, \quad i = 1, 2, \cdots 2M.$$

Once this system is solved, we take as the approximation for $u(x,t_n)$, for $n=1,\cdots,N$, the following expression

$$u^n(x) = u_h^n(x,t_n) = \sum_{j=M}^{2M} c_j^n \Psi_j(x).$$

As we will see, as **E-SD** and **E-GBF** methods, the last method controls the oscillations and has less artificial diffusivity, leading to improved solutions in terms of spreading and decaying.

However, Problem (1)–(4) has the special physically important property of balance of total mass. As we will see when we describe numerical simulations, none of the methods **E-SD**, **E-GBF**, **S-T-SD** is good at preserving such property. The next subsection explains such property and a method to improve the performance of the last procedure in this respect.

3.1 MASS CONTROL

For simplicity of exposition we take $g \equiv 0$ in (2); the general case can be similarly treated. Observe that integrating (1) on Ω, using the divergence theorem and the boundary informations, we get

$$\frac{\partial}{\partial t}\int_\Omega u dx + \int_{\partial\Omega_+} u\vec{\beta}\cdot\vec{\eta} ds = \int_\Omega f dx, \tag{18}$$

which means that the total mass of the exact solution u must satisfy the above balance equation. In particular, while the support of u does not touches the outlet part of the boundary, $\partial\Omega_+$, we must have $\dfrac{\partial}{\partial t}\int_{\tilde{\Omega}} u(x,t)dx = \int_\Omega f dx$, and, when $f\equiv 0$, the total mass must be conserved.

To improve the performance of the previous method with respect to the balance of mass, we proceed as follows. We will introduce an additional term to the right-hand side of (17) that will force the approximate solution obey a discretized version of (18). There are several ways to do that, but for simplicity we show a crude one that already improves significantly the balance of mass.

By calling M_n the total mass ($M_n = \int_\Omega u(x,t_n)dx$) carried by the solution at time t_n and using finite differences in (18), we obtain the following relation to predict the total mass that we should at each time step:

$$M_n = M_{n-1} + k_n \int_{\partial\Omega} u(x,t_n)\vec{\beta}(x)\cdot\eta(\vec{x})ds + k_n\int_\Omega f(x,t_n)dx. \tag{19}$$

On the other hand, the actual mass associated to approximate solution to be computed using finite elements is

$$\tilde{M}_n = \int_\Omega u^n(x)dx. \tag{20}$$

Thus, to force the approximate solution to follow the values of total mass that it should have, we introduce at the right-hand side of the equation the following term:

$$-\epsilon(\tilde{M}_n - M_n)\max\{u^{n-1}(x), 0\}, \tag{21}$$

for $x \in \Omega$, and where ϵ is a strictly positive constant and M_n and $\tilde{M}_n$ are computed respectively by (19) and (20). Thus, this term works either as a sink of mass when $\tilde{M}_n > M_n$ or a source when $\tilde{M}_n < M_n$. When $\tilde{M}_n = M_n$, the above term does not affect the solution. By doing this, and working as in the previous subsection, we obtain the following problem for the approximate solution:

$(\mathcal{V}_h)$ Find $u_h^n \in V_h^{0n},\ n = 1, 2, \cdots N$, such that for all V_h^{0n} there holds

$$\begin{aligned}
&\langle \frac{\partial u_h^n}{\partial t} + \vec{\beta}\cdot\nabla u_h^n, v + \delta(\frac{\partial v}{\partial t} + \vec{\beta}\cdot\nabla v)\rangle^n + \langle 3c(u_-^{n-1})^2\nabla u_h^n, \nabla v\rangle^n \\
&- \langle \text{ div } (3c(u_-^{n-1})^2\nabla u_h^n), \delta(\frac{\partial v}{\partial t} + \vec{\beta}\cdot\nabla v)\rangle^n + \langle\langle u_+^n, v_+\rangle\rangle^{n-1} \\
&= \langle f - \epsilon(\tilde{M}_n - M_n)\max\{u_-^{n-1}, 0\}, v + \delta(\frac{\partial v}{\partial t} + \vec{\beta}\cdot\nabla v)\rangle^n + \langle\langle u_-^{n-1}, v_+\rangle\rangle^{n-1}.
\end{aligned}$$

As before, the parameter δ is given by (16)

As we will see in the next section, this adaptation, which we call **Space-Time Streamline Diffusion with Mass Control**, or simply **S-T-SD-MC** for short, significantly improves the performance of method (**S-T-SD**).

4 NUMERICAL EXPERIMENTS

To show the performance of the previously describe methods, in this section we consider numerical simulations of problem (1)–(4) in very simple situations. The idea here is to make explicit the behavior of the methods, and to show the superiority of **S-T-SD-MC**.

Situation 1:

We consider a case in which an exact solution is known, and thus we have absolute control of the situation and can compare the performance of the methods in an objective way.

For this, consider the velocity field $\vec{\beta} = (1, 0)$ in a open channel of length 7 and width 2 (see Figure 1), and for the numerical simulation we use the data showed in Table 1.

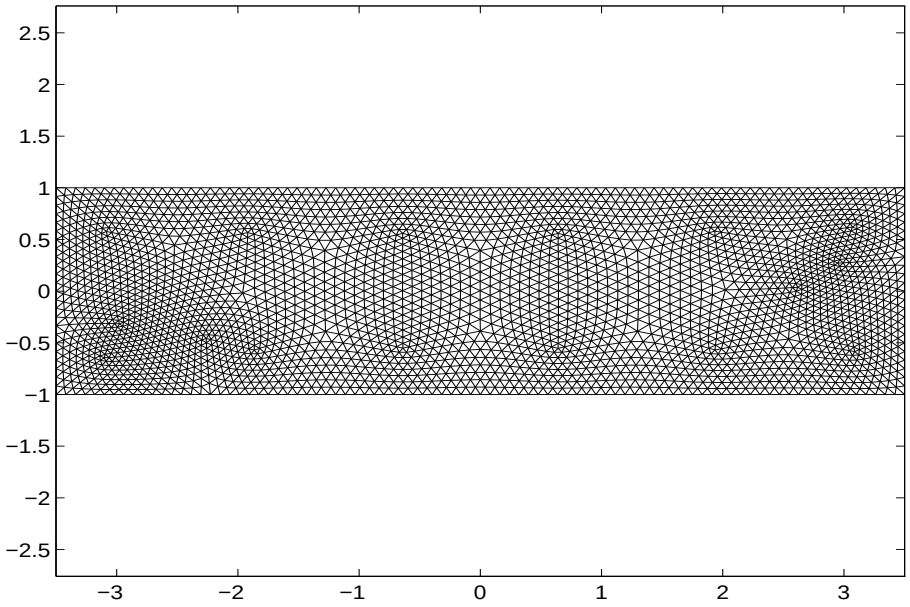

Figure 1: Open channel in Situation 1 with finite elements mesh

In this case, using results of Bertsch citeBertsch, it can be seen that an exact solution of problem (1)–(4) is given by

$$u(x,t) = v(x - \vec{\beta}t, t),$$

where

$$v(x,t) = (t+1)^{-\frac{1}{3}} \left[\max\{a^2 - \frac{1}{18}(x^2+y^2)(t+1)^{-\frac{1}{3}}, 0\}\right]^{\frac{1}{2}}.$$

Here the parameter $a > 0$ has to be chosen such that the support of u does not touch the lateral boundaries of the channel.

The performed numerical experiments showed that the **E-SD** and **E-GBF** methods have enough stability to control the oscillations presented in the standard method. However, this was obtained at expense of having excessive numerical dissipation, as it can be seen by the results presented in

Table 1: Data and parameters for the open channel problem corresponding to Situation 1

Parameters	**Values**
c	1.0
$\vec{\beta}(x,t)$	$(1,0)$
f	0.0
g	0.0
k (time stepsize)	5×10^{-2}
$u_0(x,y)$	$\left[\max\{a^2 - \frac{1}{18}(x^2+y^2), 0\}\right]^{\frac{1}{2}}$
a	0.25
Ω	$[-3.5, 3.5] \times [-1, 1]$
No. of elements (first order)	5888
No. of nodes	3057
h	0.069
$\overline{c}$	0.5
ϵ (mass control)	5×10^{-3}

Table 2, where it is clear an excessive decay of the approximate solutions, that become worse with time, obtained by those methods. **S-T-SD-MC** has good agreement with the exact values.

Table 2: Maximum values for the solutions

Method	**t = 0.5**	**t = 1**	**t = 1.5**	**t = 2**	**t = 2.5**	**t = 3**
Exact	0.2184	0.1984	0.1842	0.1733	0.1646	0.1574
E-SD	0.2064	0.1748	0.1554	0.1492	0.1289	0.1135
E-GBF	0.2064	0.1748	0.1554	0.1492	0.1289	0.1135
S-T-SD	0.2163	0.1945	0.1835	0.1744	0.1623	0.1558
S-T-SD-MC	0.2181	0.1988	0.1839	0.1739	0.1641	0.1570

We remark that it is no coincidence that the values given by the **E-SD** and **E-GBF** are very similar; the other tables and simulations show similar results. In fact, these two methods have close relation, and in Franca, Brezzi,

Bristeau, Mallet & Roge [3], a proof of their equivalence can be found. Thus, one could say that what could determine the possible choice between these two methods is their respective computational load. If one uses the same interpolation space for both methods, the first of them has more terms in its bilinear form, which leads to a greater number of integrations that have to be performed; the second method results in a larger linear system to be solved. In specific situations, one that intends to use one of these methods should take these aspects in consideration to make his choice.

Figures 2, 3 and 4 on next page show respectively the supports of the exact and the computed solutions, with **E-SD** and **S-T-SD-MC**. The support computed using **E-SD** is excessively spread; that computed using **S-T-SD-MC** has a good agreement with the exact one.

Now we pay attention to the performance of the methods with respect to the property of balance of mass. Since in the conditions of the present simulation the total mass should be preserved, a measure of the deviation of such property can obtained by the quocient between the initial total mass (**im**) and the total mass (**tm**) computed at the time of larger deviation from the initial mass. The result of this procedure applied to each of the methods is depicted in Table 3.

Table 3: Balance of mass for each method

Method	**tm/im**
E-SD	1.09384
E-GBF	1.09362
S-T-SD	1.06232
S-T-SD-MC	1.00057

We observe that the perfomances of **E-SD** and **E-GBF** are similar, as they should be according to our previous remarks, and poorer than that of **S-T-SD**, confirming the fact that this last method presents less numerical diffusion than the first two. However, **S-T-SD-MC** performs better by two orders of magnitude than the other methods.

We should also stress that **S-T-SD-MC** is better than the other methods in the important aspect of the control of the spurious oscillations, whose amplitude are much less than the ones presented by the other methods.

The following tables furnish an idea of the dependence of **S-T-SD-MC**

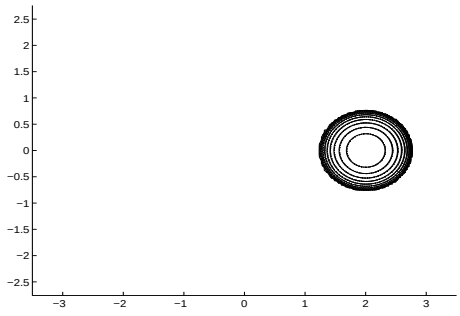

Figure 2: Exact support at $t = 2$ in the open channel problem

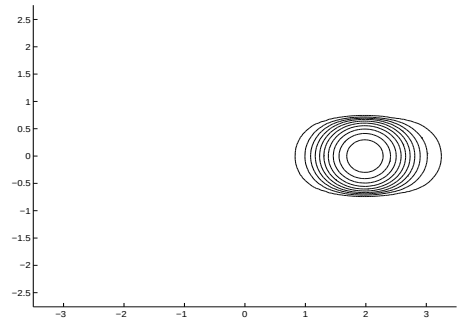

Figure 3: Support computed with (**E-SD**) at $t = 2$ in the open channel problem

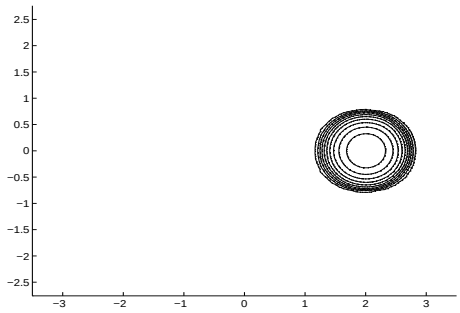

Figure 4: Support computed with (**S-T-SD-MC**) at $t = 2$ in the open channel problem

on the parameter $\overline{c} > 0$ appearing in the definition of δ given in (16). As we see from Table 4, the value of $\overline{c}$ is related the amount of numerical diffusion of the method: preserving all the other data and parameters, by increasing the value of $\overline{c}$, the amount of diffusion increases.

Table 4: Maximum values of the exact solution compared with the corresponding values of the approximate solutions

-	**t = 0.5**	**t = 1**	**t = 1.5**	**t = 2**	**t = 2.5**	**t = 3**
Exact	0.2184	0.1984	0.1842	0.1733	0.1646	0.1574
$\overline{c} = 0.5$	0.2181	0.1988	0.1839	0.1739	0.1641	0.1570
$\overline{c} = 1.0$	0.2172	0.1963	0.1831	0.1728	0.1639	0.1564

On the other hand, the maximum absolute value of the error between the exact solution and the approximation is, in this case, rather insensitive to $\overline{c}$. This can be seen in Table 5.

Table 5: Absolute error between the exact and approximate solutions

-	**t = 0.5**	**t = 1**	**t = 1.5**	**t = 2**	**t = 2.5**	**t = 3**
$\overline{c} = 0.5$	0.00266	0.00278	0.00282	0.00287	0.00349	0.00445
$\overline{c} = 1.0$	0.00266	0.00278	0.00282	0.00287	0.00349	0.00445

Situation 2:

For the next numerical experiment, we consider a situation without exact solution but still very simple. The objective is to estimate how the methods behave under the influency of non constant velocity fields. We still consider the previous open channel, but now the usual parabolic profile velocity field. The data and parameters for this numerical experiment is given in Table 6.

Figure 5 furnishes the supports of the corresponding approximate solutions computed at time $t = 6$ by using methods **E-SD** and **E-GBF**. Figure 6 gives the corresponding data for methods **S-T-SD** and **S-T-SD-MC**.

As we can see, the interplay between variations in the velocity field and the deficiencies of methods **E-SD** and **E-GBF** distorce significantively the

Table 6: Data and parameters for the open channel problem corresponding to Situation 2

Parameters	**Values**
c	1×10^{-3}
$\vec{\beta}(x,t)$	$(1-y^2, 0)$
f	0.0
g	0.0
k (time stepsize)	5×10^{-2}
$u_0(x,y)$	$0.1exp(-16((x+2.5)^2+y^2))$
Ω	$[-3.5, 3.5] \times [-1, 1]$
No. of elements (first order)	5888
No. of nodes	3057
h	0.069
$\overline{c}$	0.5
ϵ (mass control)	5×10^{-3}

support of the solution, again due to their excessive numerical diffusion. **S-T-SD-MC** behaves better, but still has excessive diffusion. **S-T-SD-MC** furnishes a reliable support in the same situation.

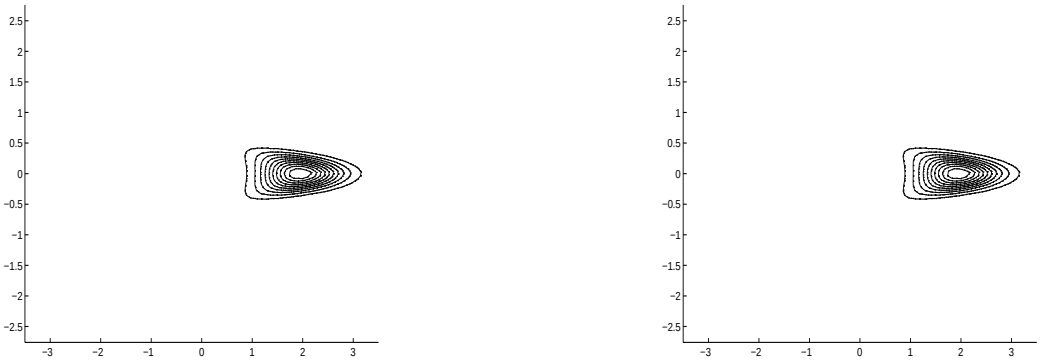

Figure 5: Support computed using **E-SD** (left) and **E-GBF** (right) in Situation 2

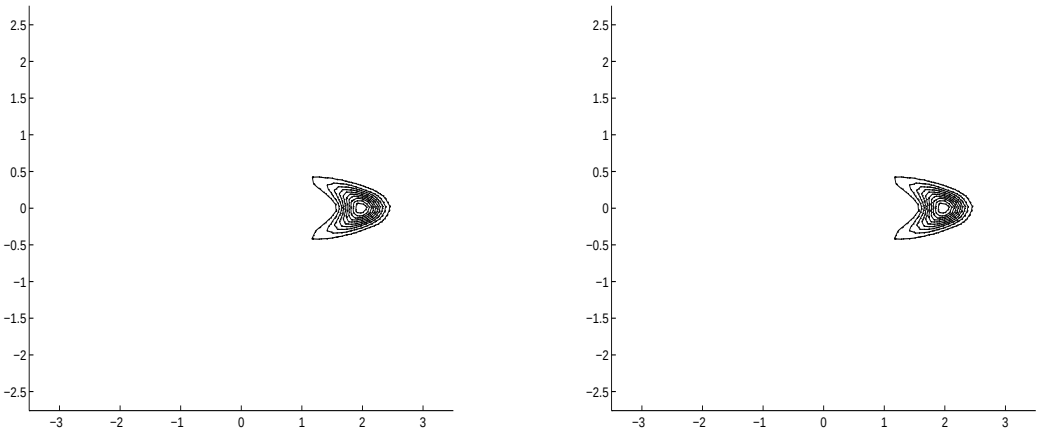

Figure 6: Support computed using **S-T-SD** (left) and **S-T-SD-MC** (right) in Situation 2

Situation 3:

The next situation considers an oil spill touching an island as it is convected by the flow. We consider the very simple case where the same channel as before contains a circular island (in this case the velocity field can also be obtained in closed form.) The corresponding domain and finite elements mesh are shown in Figure 7.

The data and parameter used in this numerical experiment are the ones in Table 7.

The performance of each of the previous methods in interaction with interior boundaries can then be evaluated by computing their behavior with respect to the conservation of total mass.

In Figs. 8, 9 and 10 we showed the behavior of the total mass along the time as computed using respectively **E-SD**, **S-T-SD** and **S-T-SD-MC**. The behavior of **E-GBF** is similar to that of **E-SD**. As we can clearly see, when the spill interacts with the boundaries of the island, conservation of mass is significatively violated for methods **E-SD** and **S-T-SD** (and also **E-GBF**). Method **S-T-SD-MC** neatly preserves the total mass in such interactions. The final decay of mass is due to the fact that at those times the spill is leaving the computational domain.

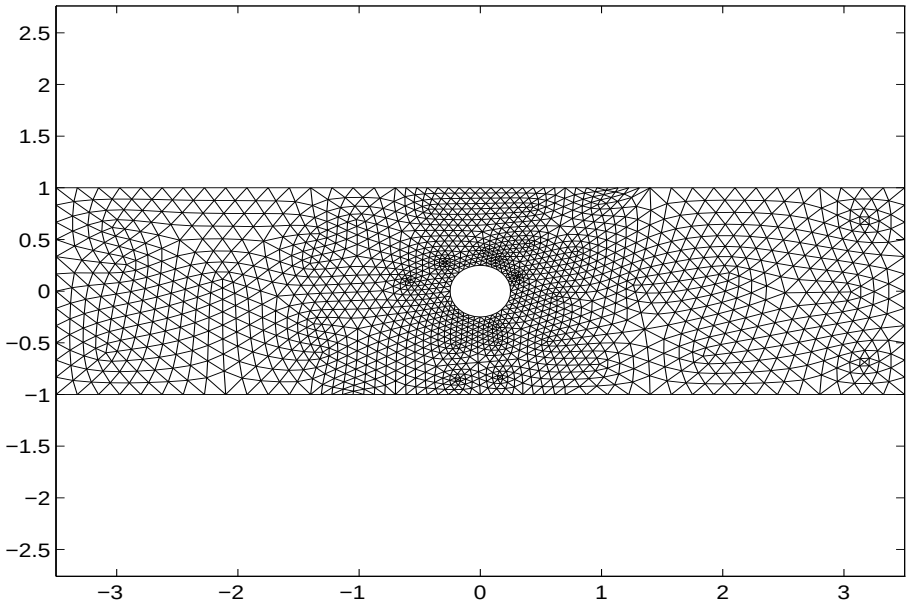

Figure 7: Domain and finite elements mesh for Situation 3

Table 7: Data and parameters for the channel with an island (Situation 3)

Parameters	**Values**
c	1×10^{-3}
$\vec{\beta}(x,t)$	$\left(1 - \frac{2x^2r^2}{(x^2+y^2)^2} + \frac{r^2}{(x^2+y^2)}\ ,\ -\frac{2xyr^2}{(x^2+y^2)^2}\right)$
f	0.0
g	0.0
k (time stepsize)	5×10^{-2}
$u_0(x,y)$	$0.1exp(-16((x+2.5)^2+y^2))$
Ω	$[-3.5, 3.5] \times [-1, 1]$
No. of elements (first order)	3520
No. of nodes	1840
h	0.088
$\overline{c}$	0.5
ϵ (mass control)	5×10^{-3}

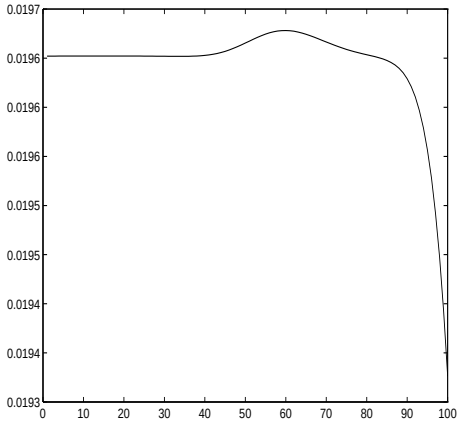

Figure 8: Total mass along the time computed using **E-SD** in Situation 3

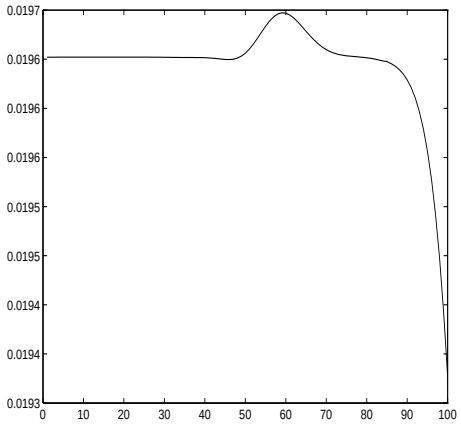

Figure 9: Total mass along the time computed using **S-T-SD** in Situation 3

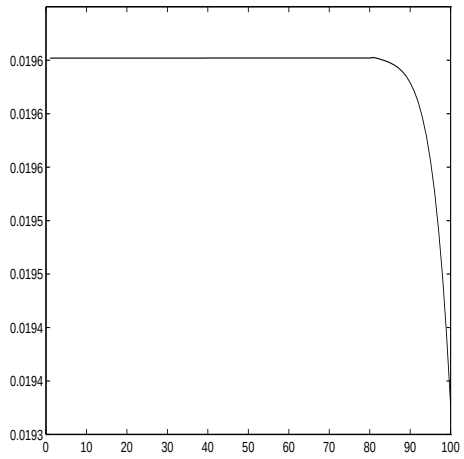

Figure 10: Total mass along the time computed using **S-T-SD-MC** in Situation 3

5 CONCLUSIONS

All the numerical experiments showed that for the problem at hand the performance of the **S-T-SD-MC**-method is better than that of the other methods in terms of quality of approximations. In particular, this is clearly so with respect to balance of mass. This method could be quickly adapted to other situations, like those that include fractional evaporation, for instance, in which the effective rate of evaporation depends on the area associated to the spill, and thus should be correctly computed. Also, by taking profit of the property of perservation of compact support of solutions, it is possible to devise a localization technique that applied to **S-T-SD-MC** can significatively reduce the size of the linear systems to be solved and, consequently, also reduce the computational time. Our conclusion is that **S-T-SD-MC** is a reliable method to be used in realistic simulations of spreading of oil spills, once it is coupled with suitable flow simulators. All these aspects will be subjets of forthcoming papers.

References

[1] J.P. Benqué, A. Hauguel & P.L. Viollet, *Engineering Application of Computational Hydraulics*, Pitman Advanced Publishing Program, London, 1982

[2] M. Bertsch, *Nonlinear Diffusion Problems: The Large Time Behavior*, Ph.D. Thesis, University of Leiden, Holland, 1983.

[3] L.P. Franca, F. Brezzi, M.O. Bristeau, M. Mallet & G. Rogé, A relationship between stabilized finite element methods and the Galerkin method with bubble functions, Computer Methods in Applied Mechanics and Engineering, n. 96, pp. 117-129, 1992

[4] L.P. Franca & C. Farhat, Bubble functions prompt unusual stabilized finite element methods, Computer Methods in Applied Mechanics and Engineering, n. 123, pp. 299-308, 1995

[5] C. Johnson, *Numerical solution of partial differential equations by the finite element method*, Cambridge University Press, Cambridge, 1987.